JOURNAL OF THERMOPHYSICS AND HEAT TRANSFER
Vol. 20, No. 4, October–December 2006

Thermal Analysis for Propellant Stream in Thruster's Injection Tube During Start Process

Ze-juan Xiao* and Hui-er Cheng†
Shanghai Jiao Tong University, 200030 Shanghai, People's Republic of China

DOI: 10.2514/1.19089

According to the leading design features of the monopropellant attitude-control thruster and the cryogenic condition in space, the coupling heat-transfer physical model and a set of mathematical equations are put forward to calculate the temperature variation of the injection tube and three other components of the thruster, which are the aggregate organ, the bracket, and the injection plate. The wall temperature of the injection tube is taken as the thermal boundary conditions for the propellant stream temperature drop calculation. The temperature calculation of the propellant stream flowing inside the injection tube during the start process in a typical 10 N thruster has been performed, and two simulation experiments are carried out on the same type thruster in the vacuum cryogenic chamber. The results of the calculation agree well with the experiments. The validated calculation model can be used to judge whether the propellant stream freezes or not in the injection tube during the start process after the thruster has been exposed to the cryogenic space for a long time. In addition, four factors that affect the front temperature of the propellant stream at the injection tube exit during the propellant filled process are studied, and according to the calculation results, three correlation relationships are deduced, respectively.

Nomenclature

C	=	specific heat, $J/(K \cdot kg)$
d_{out}, d_{in}	=	outer diameter and inner diameter of the injection pipe, m
E	=	emissive power of each component of the thruster, W/m^2
E_{be}	=	Earth infrared constant, 220 W/m^2
F_1	=	area of the aggregate-organ's surface, m^2
f	=	area of the injection-tube's exterior surface at node n, m^2
H	=	altitude of the orbit, km
h	=	convection heat-transfer coefficient, $W/(m^2 \cdot K)$
J	=	effective radiation intensity, W/m^2
L	=	length of the injection tube, m
l	=	length of the injection-tube element, m
n	=	node number of the injection tube
Q	=	heat fluxes, W
R	=	surface radiation thermal resistance, $1/m^2$
T_0	=	initial temperature of each component of the thruster, K
T_1, T_2, T_3	=	temperature of the aggregate organ, the injection plate, and the bracket, K
T_n^i	=	temperature of the injection-tube node n, K
t_n^l	=	temperature of the propellant stream element, K
t_i	=	freezing point temperature of the propellant, K
t_{in}	=	temperature of the propellant at the entry of the injection tube, K
t_{out}	=	front temperature of the propellant stream at the exit of the injection tube, K
u	=	propellant flow velocity in the injection tube, m/s
X	=	radiation view factor
α	=	absorptance of the thruster's components to the Earth's infrared radiation
α'	=	radiation equivalent heat-transfer coefficient
$\Delta\tau$	=	time step, s
ε	=	surface emissivity of each component of the thruster
η	=	dynamic viscosity, $Pa \cdot s$.
θ	=	angle between thruster's axis and the Earth
λ	=	thermal conductivity, $W/(m \cdot K)$
ρ	=	density, kg/m^3
σ	=	Stefan–Boltzmann constant, 5.67×10^{-8} $W/(m^2 \cdot K^4)$
τ	=	time (the fairing is thrown away at $\tau = 0$ and the thruster is started at $\tau = \tau_0$), s
Nu	=	Nusselt number
Pr	=	Prandtl number
Re	=	Reynolds number

Subscripts

e	=	Earth
n	=	node index
0	=	space cryogenic environment
1	=	aggregate organ
2	=	injection plate
3	=	bracket

I. Introduction

THERMAL reliability research is one of the key steps in the rockets and spacecrafts' designing. The accidents induced by the thermal control malfunction are not infrequent and these accidents sometimes lead to the rockets being damaged and the satellites smashed [1,2]. The attitude-control thrusters of the upper stage in the launch vehicle CZ-2C/FP are small monopropellant engines. According to the fixed procedure, these attitude-control thrusters must be exposed to the space cryogenic environment for a long time after the fairing is thrown away, so that the temperature of the thruster's components will drop greatly as the heat radiates into space continuously; however, the temperature cannot be adjusted by the initiative method [3]. The inner diameter of the injection tube of the thruster is around 0.5 mm or less; the propellant will probably freeze while flowing through the injection tube and will not enter the chamber, and then the thruster system will fail to start and its mission will end [4,5]. As stated previously, the thermal reliability of the thruster during the start process in the space cryogenic environment

Received 25 July 2005; revision received 25 October 2005; accepted for publication 26 October 2005.

*Ph.D. Student, Department of Aeronautics and Astronautics. Member AIAA.
†Full Professor, Department of Aeronautics and Astronautics.

is a key problem of the reliability of the whole rocket. It has drawn great attention from the designers all along [6,7].

To judge the thermal reliability of the thruster when it is started, the temperature variation of the propellant flowing through the injection tube must be known clearly. The temperature drop rate of the propellant is directly correlative with the wall temperature of the injection tube, and so the wall temperature distribution characteristic of the injection tube should be obtained at the first step. After the propellant enters the injection tube, there are three heat fluxes acting on the injection-tube node n: the conduction heat transfer with the adjacent elements, the convection heat transfer with the propellant, the radiation heat transfer with the ambient components in the thruster and the space cryogenic environment. To solve this complicated problem, several physical assumptions are put forward and the coupling heat transfer among the thruster's components, the space cryogenic environment, and the propellant stream has been calculated.

II. Physical Model

As shown in Fig. 1, the temperature calculation of the monopropellant attitude-control thruster mainly involves the heat transfer calculating among the injection tube, the aggregate organ, the bracket, and the injection plate of the thruster. To show the main aspect of the complicated problem, seven physical assumptions were presented: 1) The thruster is in the shade area, the temperature of the space cryogenic environment T_0 is about 4 K, and the pressure is about 1.68×10^{-7} Pa, and so the sunlight radiation and the air convection heat transfer need not be taken into account. The initial temperature of each component of the thruster is 293 K at time $\tau = 0$, when the fairing is thrown away. 2) In the temperature drop calculation of the aggregate organ, the bracket, and the injection plate, the three objects are treated as zero-dimensional temperature distribution approximately. It is considered that they release heat into the cryogenic environment and receive heat of infrared radiation from the Earth separately. The heat transfer among these three components is not considered and the inappreciable heat flux from the small injection tube is also neglected. 3) The left side of the aggregate organ is connected with an electromagnetism valve by a heat insulator, and the right side of the injection plate is connected with a closed space, so that both sides can be approximately dealt with in the adiabatic condition. 4) In the temperature drop calculation of the injection tube, the radiation heat transfer between the injection tube and the aggregate organ, the bracket as well as the injection plate is taken into account; the radiation heat loss into the cryogenic environment through four trapezium windows on the bracket is also calculated. The radiation heat coming from the Earth is not considered because most of the heat is kept out of the bracket. 5) Because the temperature distribution of the aggregate organ, the bracket, and the injection plate is not the concerned emphasis while analyzing their influence on the temperature drop of the injection tube, the three objects are approximately treated as zero-dimension temperature distribution in this paper. 6) Because the injection-tube wall is very thin, only 0.15 mm, the temperature difference in radial is undoubtedly neglected. The heat transfer of the injection tube is taken as a one-dimension longitudinal instantaneous heat conductive problem.

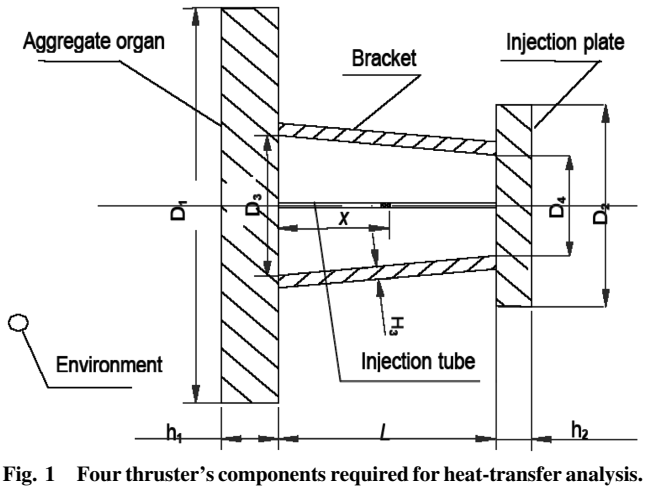

Fig. 1 Four thruster's components required for heat-transfer analysis.

At the time of $\tau = \tau_0$, the attitude-control thruster is started, and the propellant is injected into the injection tube from the storage tank (not shown in Fig. 1), and it flows toward the combustion chamber (also not shown in Fig. 1). In the convection heat-transfer calculation between the propellant and the thin wall of the injection tube, the physical assumptions are the following: 1) According to the character of the engineering demand, it is taken as a one-dimensional flow and heat-transfer problem, the radial temperature distribution of the propellant stream has not been considered, and the axial conduction heat transfer is neglected. 2) The inner diameter of the injection tube $d_{\text{in}} > 0.2$ mm and the propellant is the incompressible liquid, the flow is in the continuum regime, and so the Navier–Stokes equations and the conventional convection heat-transfer relationships are selected to describe the fluid motion and convection heat transfer [8–11].

III. Heat-Transfer Equations

A. Temperature Calculation Formulas of the Aggregate Organ, the Bracket, and the Injection Plate

The temperature of the aggregate organ, the bracket, and the injection plate is expressed as T_1, T_2, and T_3, respectively. Because their calculation method and the physical character parameters of the three components are the same, only the calculation of the aggregate organ is specified here.

According to previous physical assumptions, the relationship of the energy conservation about the aggregate organ can be expressed as follows:

$$\begin{aligned}&\text{received heat from the infrared radiation of the Earth } Q_{\text{rec}}\\ &\quad - \text{radiation heat loss into the cryogenic environment } Q_{\text{los}}\\ &\quad = \text{energy increase } Q_{\text{inc}}\end{aligned} \tag{1}$$

Writing the above heat flux expression formulas and substituting them into the relationship (1), the transient temperature of the aggregate organ can be calculated through the following equation:

$$T_1^{i+1} = T_1^i - \frac{\varepsilon_1 \sigma \Delta\tau}{\rho_1 C_1 V_1}(T_1^i)^4 + \frac{\alpha_1 E_{\text{be}} X_{1,e} F_1}{\rho_1 C_1 V_1}\Delta\tau \tag{2}$$

where T_1^{i+1} and T_1^i are the temperature of the aggregate organ at the time of $i+1$ and i, α_1 is the absorptance of the surface to the Earth's infrared radiation, and ε_1 is the surface emissivity of the aggregate organ. According to the thermal controlling theory of the spacecraft, the Earth is usually considered as a blackbody with temperature of $T = 250$ K [12], so $E_{\text{be}} = 220$ W/m^2. And $X_{1,e}$ is the radiation view factor of the aggregate-organ surface F_1 to the Earth [12–14]. Its value depends on the altitude H of the orbit and the angle θ between the thruster's axis and the Earth, σ is the Stefan–Boltzmann constant, ρ_1, C_1, and V_1 express the density, the specific heat, and the volume of the aggregate organ, respectively.

The transient temperature calculation equations of the bracket and the injection plate can be deduced in the same way, and they have the same form as follows:

$$T_2^{i+1} = T_2^i - \frac{\varepsilon_2 \sigma \Delta\tau}{\rho_2 C_2 V_2}(T_2^i)^4 + \frac{\sigma_2 E_{\text{be}} X_{2,e} F_2}{\rho_2 C_2 V_2}\Delta\tau \tag{3}$$

$$T_3^{i+1} = T_3^i - \frac{\varepsilon_3 \sigma \Delta\tau}{\rho_3 C_3 V_3}(T_3^i)^4 + \frac{\sigma_3 E_{\text{be}} X_{3,e} F_3}{\rho_3 C_3 V_3}\Delta\tau \tag{4}$$

B. Temperature Calculation Formula of the Injection Tube Before the Thruster Started

As shown in Fig. 1, the injection tube with the length of L is divided into N elements along the axis. To choose the node n which is x mm away from the aggregate organ as the researching object, the conservation equation of energy is

$$\text{received heat by conduction } Q_{n,\text{rec}} - \text{heat loss by radiation } Q_{n,\text{los}} = \text{energy increase } Q_{n,\text{inc}} \quad (5)$$

where the heat flux $Q_{n,\text{los}}$ is the radiation heat transfer between the injection tube and other four objects, namely, the aggregate organ, the bracket, the injection plate, and the cryogenic environment. The calculation of the conduction heat transfer $Q_{n,\text{rec}}$ and increased energy $Q_{n,\text{inc}}$ is simpler as compared to the radiation heat transfer $Q_{n,\text{los}}$, so that only the calculation method of $Q_{n,\text{los}}$ is specified below.

The simplified thermal radiation network is shown in Fig. 2. $E_{n,b} = \sigma(T_n^i)^4$ is the emissive power of element n, $R_n = (1-\varepsilon)/(\varepsilon f)$ is the surface radiation thermal resistance, ε is the surface emissivity of the injection tube, $f = \pi d_{\text{out}} l$ is the exterior area of the node n, d_{out} is the outer diameter of the injection tube, $l = L/N$ is the length of the node, J_n, J_1, J_2, J_3, and J_0 are the effective radiation intensity of the node n, the aggregate organ, the bracket, the injection plate, and the cryogenic environment, respectively, $R_{n,1} = 1/(fX_{n,1})$, $R_{n,2} = 1/(fX_{n,2})$, $R_{n,3} = 1/(fX_{n,3})$, and $R_{n,0} = 1/(fX_{n,0})$ are the space radiation thermal resistance between J_n, and J_1, J_2, J_3, J_0. The radiation view factors between the node n and the aggregate organ, the bracket, the injection plate, and the four trapezium windows are $X_{n,1}, X_{n,2}, X_{n,3}$, and $X_{n,0}$, and $E_{b1} = \sigma(T_1^i)^4$ is the emissive power of the aggregate organ.

The area $1/4\pi D_3^2$ on the aggregate-organ surface in calculating $X_{n,1}$ is much larger than f which is the exterior area of node n, and the emissivity $\varepsilon = \varepsilon_1$, so that the surface radiation thermal resistance $R_1 = (1-\varepsilon_1)/(\varepsilon_1 1/4\pi D_3^2)$ can be neglected in comparison with R_n, and then the approximate equation $J_1 = E_{b1}$ is obtained. Similarly, $J_2 = E_{b2} = \sigma(T_2^i)^4$, $J_3 = E_{b3} = \sigma(T_3^i)^4$, and $J_0 = E_{b0} = \sigma(T_0)^4$.

Based on Kirchhoff's law, the radiation heat loss $Q_{n,\text{los}}$, of the injection-tube node n can be expressed as

$$Q_{n,\text{los}} = \frac{E_{n,b} - J_n}{R_n} \quad (6)$$

$$Q_{n,\text{los}} = \frac{J_n - J_1}{R_{n,1}} + \frac{J_n - J_2}{R_{n,2}} + \frac{J_n - J_3}{R_{n,3}} + \frac{J_n - J_0}{R_{n,0}} \quad (7)$$

According to the assumption in the above physical model, the tiny thermal effect of the injection tube is neglected while calculating the temperature of the aggregate organ, the injection plate, and the bracket. The temperatures of the aggregate organ T_1^i, the bracket T_2^i, and the injection plate T_3^i have already been obtained by Eqs. (2–4) before calculating the temperature T_n^i; that is to say, J_1, J_2, and J_3 are available in Eq. (7). In addition, the temperature T_0 of the space cryogenic environment is assumed as 4 K, so $J_0 = \sigma(T_0)^4 = 4$. Calculating Eqs. (6) and (7), the heat flux $Q_{n,\text{los}}$ is expressed as follows:

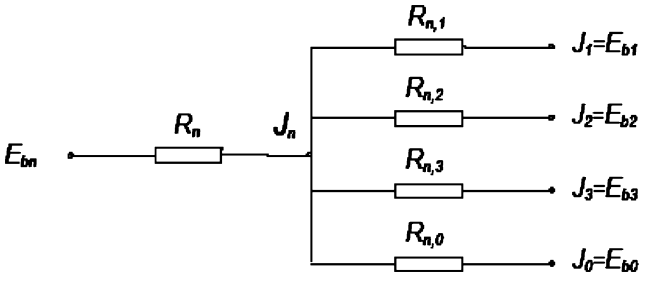

Fig. 2 Simplified thermal radiant network of the injection-tube node n.

$$Q_{n,\text{los}} = \varepsilon f \sigma\{(T_n^i)^4 - [(T_1^i)^4 X_{n,1} + (T_2^i)^4 X_{n,2} + (T_3^i)^4 X_{n,3}]\} \quad (8)$$

Putting each of the energy expressions into Eq. (5), the temperature of the point of time $i+1$ is written as

$$T_n^{i+1} = T_n^i + \frac{\Delta\tau}{\rho C \Delta V}\left\{\frac{\lambda F}{l}(T_{n+1}^i + T_{n-1}^i - 2T_n^i) - \varepsilon f \sigma_0 (T_n^i)^4 + \varepsilon f \sigma_0 [(T_1^i)^4 X_{n,1} + (T_2^i)^4 X_{n,2} + (T_3^i)^4 X_{n,3}]\right\} \quad (9)$$

where $\Delta V = F \cdot l$ is the volume of the injection-tube element n, $F = 0.25\pi(d_{\text{out}}^2 - d_{\text{in}}^2)$ is the cross section area, and d_{in} is the inner diameter. T_{n+1}^i, T_n^i, and T_{n-1}^i are the temperature of the injection-tube element $n-1$, n, and $n+l$ at time i. λ is the thermal conductivity of the injection tube and it varies with temperature $\lambda(T) = 3.23 + 0.0626T - 7.0675 \times 10^{-5} T^2$ $(180 < T < 300$ K); the standard deviation of the simulated equation is 0.019.

As shown, the physical significance of each term in Eq. (9) is fairly clear. The injection-tube temperature of node n at time point $i+1$ depends on the temperature of node $n+1$ and $n-1$ at time point i, the temperature of the aggregate organ T_1^i, the bracket T_2^i, and the injection plate T_3^i as well as the value of the view factors that vary with the location of x are marked in Fig. 1.

C. Temperature Calculation Formula of the Propellant Stream and the Injection Tube After the Thruster Started

Once the start command of the thruster is given, the electromagnetism valve is turned on immediately, and the propellant will flow out of the storage tank and enter into the injection tube. Whether or not the propellant could flow through the injection tube without any freezing accident and arrive at the thruster chamber is a vital problem which relates to the success of the thruster start.

To avoid the freezing accident happening, the temperature of the propellant stream while flowing in the injection tube must be clear at first. Analyzing each factor that affects the temperature of the propellant stream, the energy conservation equation of the propellant stream element n is written as

$$\text{heat flux brought in by flow } Q_{p,\text{inf}} + \text{convective heat flux from the injection-tube wall } Q_{p,\text{con}} = \text{energy increase } Q_{p,\text{inc}} \quad (10)$$

Writing the above three heat flux expressions and substituting them into relationship (10), the temperature calculation equation of the propellant stream element n can be expressed as

$$t_n^{j+1} = t_n^j + \frac{u\Delta\tau_p}{l}(t_{n-1}^j - t_n^j) + \frac{h f_n \Delta\tau_p}{C_n}(T_n^{k+j} - t_n^j) \quad (11)$$

where t and T are the temperatures of the propellant stream and the injection-tube wall, n is the number index of the node, the superscripts j and $k+j$ are, respectively, the time point j and the time point $k+j$. The different superscripts j and $k+j$ represent the different time beginnings, the time point j begins at the time $\tau = \tau_0$ when the thruster is started, and the time point $k+j$ begins at the time $\tau = 0$ when the fairing is thrown. Here the value of k is obtained by an equation which is $\tau_0 = k\Delta\tau$, $\Delta\tau_p$ is the time step, $C_n = \rho_f C_f \Delta V_n$ is the thermal capacity of the propellant stream element n, ρ_f and C_f are the density and specific heat of the propellant, $\Delta V_n = 0.25\pi d_{\text{in}}^2 l$ is the volume of the propellant stream element, and $f_n = \pi d_{\text{in}} l$ is the interior area of the injection-tube element. Equation (11) can also be used to calculate the temperature of the propellant front during the start process $\tau = 0 \sim L/u$; t_n^j is then taken as the temperature of the propellant stream of previous node $n-1$ at time j.

The parameter h in Eq. (11) is the convection heat-transfer coefficient which is calculated as

$$h = Nu\frac{\lambda}{d_{\text{in}}} \tag{12}$$

Based on the physical assumptions above, in calculating the convection heat transfer where the propellant flows through the thin injection tube at low temperature, the conventional convection heat-transfer relationship is chosen. In most cases of the attitude-control thruster thermal calculation, the value range of the inner diameter of the injection tube, the velocity of the propellant, the Reynolds numbers, the Prandtl number, and the dynamic viscosity ratio are $d_{\text{in}} \in (0.2, 1.3)$ mm, $u \in (1, 15)$ m/s, $Re \in (43, 4300)$, $Pr \in (36, 88)$, and $\eta_f/\eta_w \in (0.41, 1)$, respectively.

According to the conditions above, when the Reynolds numbers $Re < 2200$, the Sieder–Tate equation [15] is chosen to calculate the Nusselt number:

$$Nu_f = \begin{cases} 1.86\left(Re\,Pr_f\frac{d_{\text{in}}}{L}\right)^{1/3}\left(\frac{\eta_f}{\eta_w}\right)^{0.14} & Re\,Pr_f\frac{d_{\text{in}}}{L} \geq 10 \\ 3.66 & Re\,Pr_f\frac{d_{\text{in}}}{L} < 10 \end{cases} \tag{13}$$

When the Reynolds numbers $Re > 2200$, the Gmelinski equation (14) is chosen to calculate the Nusselt number:

$$Nu = 0.012(Re^{0.87} - 280)Pr_f^{0.4}\left[1 + \left(\frac{d_{\text{in}}}{L}\right)^{2/3}\right]\left(\frac{Pr_f}{Pr_w}\right)^{0.11} \tag{14}$$

After the thruster is started, the convection heat flux $Q_{p,\text{con}}$ of the propellant will be added to Eq. (5), and then, the instantaneous temperature calculating Eq. (9) of the injection-tube element n is changed into:

$$\begin{aligned} T_n^{k+j+1} = T_n^{k+j} + \frac{\Delta\tau_p}{\rho\Delta VC}\Big\{&\frac{\lambda F}{l}(T_{n+1}^{k+j} + T_{n-1}^{k+j} - 2T_n^{k+j}) \\ &- \varepsilon f\sigma(T_n^{k+j})^4 + \varepsilon f\sigma[(T_1^{k+j})^4 X_{n,1} + (T_2^{k+j})^4 X_{n,2} \\ &+ (T_3^{k+j})^4 X_{n,3}] + hf_1(T_n^{k+j} - t_n^j)\Big\} \end{aligned} \tag{15}$$

To calculate the coupling equations (11) and (15), the temperature variation of the propellant stream and the injection tube can be gained from the start time $\tau = \tau_0$

IV. Temperature Drop Analysis of the Thruster's Components and the Propellant

Calculating conditions: the value of the time step is an artificial variable, in the period from when the fairing is thrown at time $\tau = 0$ to time $\tau = \tau_0$ when the thruster is started, the time step $\Delta\tau = 0.1$ s, and the time step after the thruster is started is $\Delta\tau_p = 0.1$ ms. The outer diameter of the injection tube is $d_{\text{out}} = 0.6$ mm, the inner diameter of the injection tube is $d_{\text{in}} = 0.3$ mm, the length of the injection tube is $L = 30$ mm, and the total number of the node along the tube is $N = 30$. The emissivity of each thruster's components is $\varepsilon = 0.6$, and the absorptance of the thruster's components to the Earth's infrared radiation is $\alpha = 0.6$. At the instant when the fairing is thrown, the initial temperature of each component of the thruster is 293 K.

The angle between the thruster's axis and the Earth θ is changing in flight. The calculation results have shown that the quantity of the radiation heat flux the thruster gets from the Earth will change with the angle θ, but the temperature drop rule is similar. One typical case of $\theta = 0$ is analyzed in detail and the case $\theta = \pi/2$ is mentioned briefly below. The altitude of the orbit is $H = 400$ km.

The propellant is DT3, and its property parameters can be found in a special manual. The initial temperature of the propellant when injected into the injection tube is $t_{\text{in}} = 263$ K, its freezing point is $t_{\text{in}} = 243$ K, and the velocity that the propellant flows through the injection tube is selected as $u = 1$ m/s.

A. Temperature Variation of the Thruster's Components

Figure 3 shows the temperature of the aggregate organ, the bracket, the injection plate, and the lowest temperature of the injection tube calculated in 10 h after the fairing is thrown away at time $\tau = 0$. As shown in Fig. 3, the temperature drop rate $dT/d\tau$ of these four components is quite large at the first 2 h then the temperature drop slows down little by little. The temperature difference between the aggregate organ, the injection plate, and the injection tube is quite small all along. Because the temperature drop rate of the bracket is obviously larger than the three others at the beginning, so its temperature is much lower in a longer period. The temperature of each component closes to each other in the end. Obviously, the temperature drop rate of these components depends on each time constant $\tau' = \rho CV/\alpha' F$. Three hours later, the temperature of the injection tube drops below the freezing point of the propellant TD3; if the thruster is started at this time, the propellant may freeze and the injection tube may be blocked.

Figure 4 shows axial variation of injection-tube temperature in eight different times from $\tau = 0$ to $\tau = 7200$ s with the angle $\theta = 0$. Affected by the aggregate organ and the injection plate, the temperature distribution of the injection tube is higher on both ends but lower in the middle at the beginning; then the lowest temperature location of the injection tube will move toward the injection plate whose temperature drops a little faster than the aggregate organ.

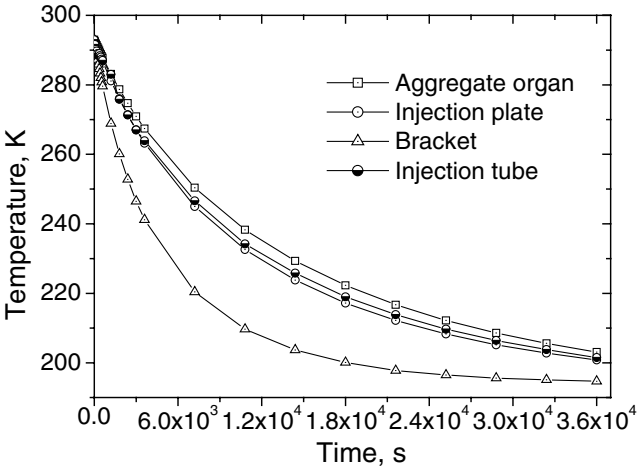

Fig. 3 Temperature variation of the thruster' components in 10 h after the fairing is thrown.

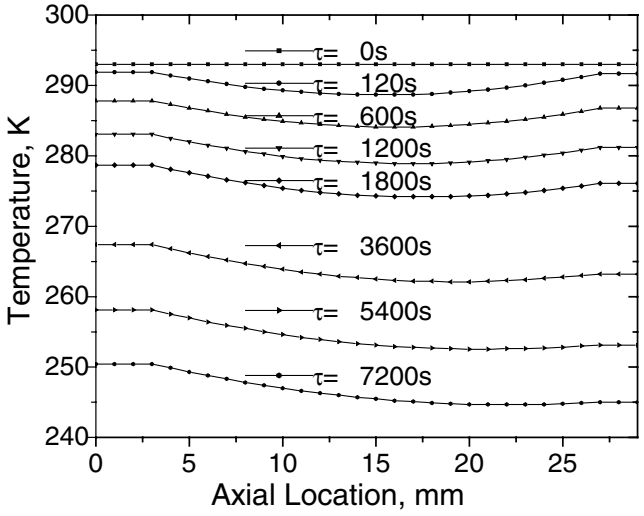

Fig. 4 Axial variation of the injection-tube temperature in 7200 s after the fairing is thrown.

B. Temperature Variation of Injection Tube and Propellant Stream Variation During Start Process

The curves in Figs. 5 and 6 express the temperature distribution of the injection tube and the propellant stream after the thruster starts at time $\tau = \tau_0 = 5000$ s. In the two figures, L/u expresses the requisite time that the propellant stream flows through all lengths of the injection tube. In the propellant filled process $0 \sim L/u$, the temperature drop range of the propellant stream is biggest, and the temperature of the propellant stream drops to the lowest point at the injection-tube exit at time $\tau = \tau_0 + L/u$. This temperature is named the front temperature t_{out}, and it is an important variable in the analysis below. As the heat flows in with the new propellant coming from the storage tank, the temperature of the injection tube rises gradually and reaches equilibrium with the propellant stream after 10 s. The temperature difference between the injection tube and the propellant stream is less than 1 K at the thermal equilibrium state. It can be seen that if the front temperature of the propellant stream t_{out} in the injection tube is higher than the freezing point t_i, the propellant can flow through the injection tube continuously without any freezing accident happening afterward.

V. Calculating Equations of Temperature t_{out} in Different Conditions

Figures 5 and 6 show that if the front temperature t_{out} of the propellant is higher than the freezing point t_i during the start process, the propellant can flow through the injection tube freely afterward and will never freeze. So the front temperature t_{out} is a key parameter in the thermal reliability research here. As shown in Eq. (11), the main factors that influence the front temperature t_{out} are the length L and the inner diameter d_1 of the injection tube, the flow velocity u and the entry temperature t_{in} of the propellant stream, and the thruster's start time τ_0.

The front temperature t_{out} for different start time τ_0 is shown in Fig. 7. The calculation condition of the thruster's components and the propellant in Fig. 7 is the same as above, the velocity of the propellant stream is 1 m/s, and the entry temperature t_{in} is 263 K. As shown in Fig. 7, the front temperature t_{out} is higher than the freezing point t, when the thruster starts at time $\tau_0 = 6$ h, that is to say, the propellant will not freeze if the thruster starts 6 h after the fairing is thrown.

Figure 8 shows that the front temperature t_{out} varies with the velocity of the propellant stream in different length L and different inner diameter d_{in}. In the calculation, the parameters of the thruster's components and the propellant properties are the same as that above, and the initial temperature of the propellant stream t_{in} is 263 K. The temperature of the injection tube at the time $\tau_0 = 7200$ s is chosen as the thermal boundary condition of the convection heat transfer.

As shown in Fig. 8, when the velocity of the flow $u \geq 4$ m/s, the front temperature t_{out} rises slowly as the velocity increases and the propellant will not freeze in all different dimensions of the injection tube, but when $u \leq 4$ m/s, the temperature drop rate of the propellant increases and the temperature becomes sensitive to the velocity of the flow. Also, the front temperature t_{out} drops as the diameter reduces and the length of the injection tube increases.

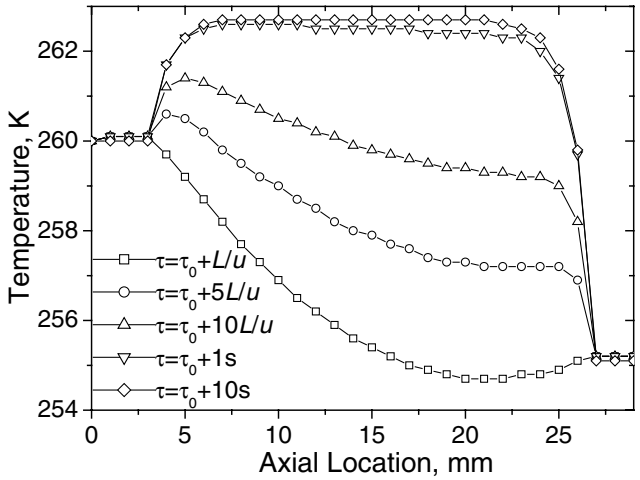

Fig. 5 Temperature variation of the injection tube in 10 s after the thruster starts.

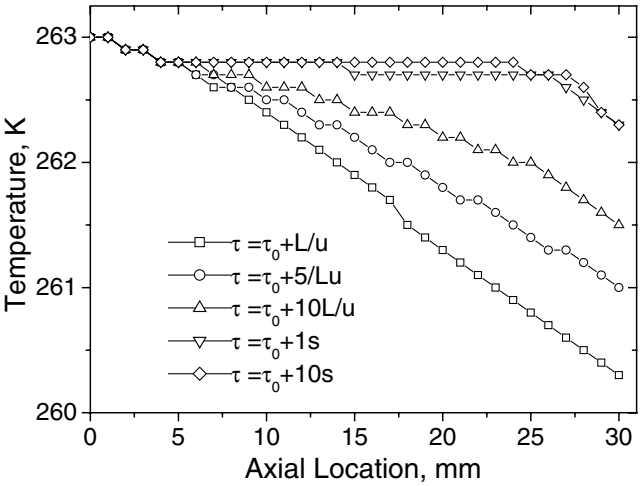

Fig. 6 Temperature variation of the propellant stream in 10 s after the thruster starts.

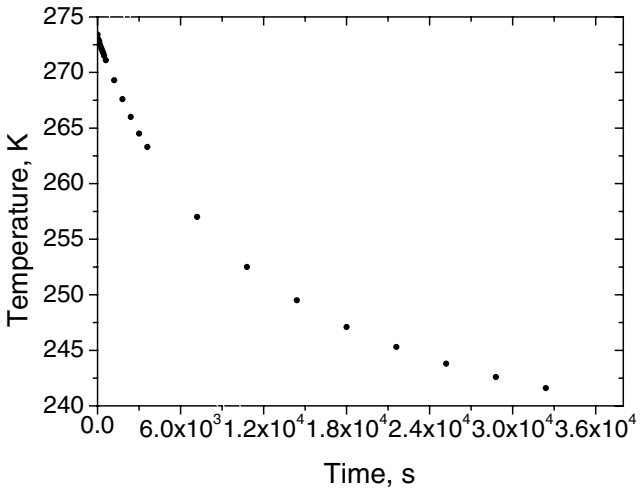

Fig. 7 Temperature t_{out} variation in 10 h after the fairing is thrown.

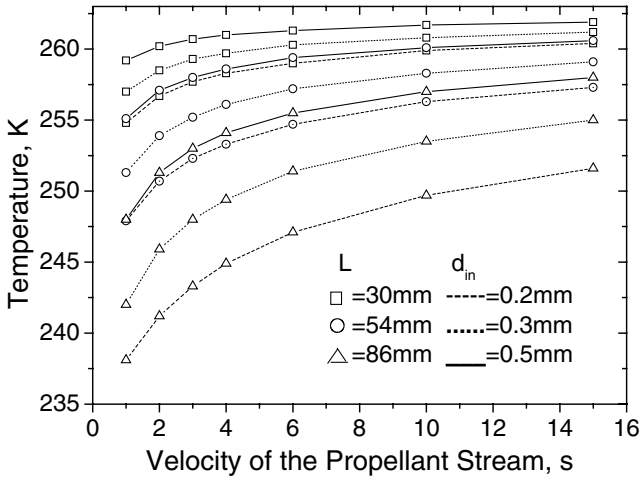

Fig. 8 Temperature t_{out} variation with the velocity of the propellant stream u in different length L and different inner diameter d_1.

Calculation results show that while the length $L < 54$ mm and the inner diameter $d_{in} > 0.2$ mm, the front temperature t_{out} is above the freezing point for all the different flow velocities.

According to the design criterion of the thruster and the demand of the flight mission, the initial temperature of the propellant in the storage is higher than 263 K and the time τ_0 is usually shorter than 7200 s. Under these conditions, the front temperature t_{out} variation with the flow velocity of the propellant stream u, the length L, and the inner diameter d_{in} of the injection tube are calculated, respectively, and these simulation correlation formulas are shown as follows:

Front temperature t_{out} varies with the velocity u:

$$t_{out} = 258.36 - 10.46e^{-0.39u} \tag{16}$$

Applicable range: $L = 54$ mm, $d_{in} = 0.3$ mm, and $u = 1$–15 m/s.

Front temperature t_{out} varies with the inner diameter d_{in}:

$$t_{out} = 259.71 - 23.39e^{-3.27d_{in}} \tag{17}$$

Applicable range: $L = 54$ mm, $u = 1$ m/s, and $d_{in} = 0.3$–1.3 mm

Front temperature t_{out} varies with the length of the tube L:

$$t_{out} = 265.2 - 0.26L \tag{18}$$

Applicable range: $d_{in} = 0.3$ mm, $u = 1$ m/s, and $L = 30$–86 mm.

The correlative coefficient is 0.99 in the formulas above, and the parameters' applicable range includes almost all the values in the thruster designing.

VI. Comparisons Between Calculation and Experimentation

To test the thermal reliability of the thruster and make sure that the propellant can flow through the injection tube and enter into the chamber without a freezing accident happening, an experiment using the 10 N thruster is carried out in the vacuum cryogenic chamber on the ground and another cryogenic experiment using the head of the thrust chamber is performed too. The simulation calculation is carried out under the experimental conditions and the results are compared with the experimentation.

A. Vacuum Cryogenic Experimentation for a 10 N Thruster

The space cryogenic simulation experiment using the 10 N thruster is performed in the KM1 vacuum chamber. Because of the space limitation, the scheme of the experimental apparatus is not included here. The experimental conditions are the following: the absolute pressure in the chamber is 1.2×10^{-2} Pa, the cryogenic medium is liquid nitrogen, and the inner wall temperature of the chamber is 100 K. As we know, the convection heat transfer can be neglected under such low pressure, and the radiant heat flux coming from the inner wall of the chamber is very weak, so that the experiment condition can be used to simulate the space cryogenic low-pressure environment.

Figure 9 compares the temperature of the aggregate organ, the injection plate, and the lowest temperature of the injection tube obtained from experimentation and the calculation under the same conditions. As can be seen, the difference between the calculation and the experimentation is less than 4 K, and this kind of deviation is acceptable in the engineering calculation. So, the thermal analysis of the monopropellant thruster in the space cryogenic environment is valuable in the thermal control designing, and the temperature calculation results of the thruster's components provide the right thermal boundary condition in calculating the propellant stream temperature variation in the injection tube.

B. Cryogenic Experiment Using the Head of the Thrust Chamber

The sketch of the experimental apparatus is shown in Fig. 10. The real propellant is replaced with the simulation liquid whose property parameters are very close to the real propellant and the freezing point is also 243 K. In the test, the injection tube is immersed in the coolant directly, and the thermal capacity of the simulation liquid flowing

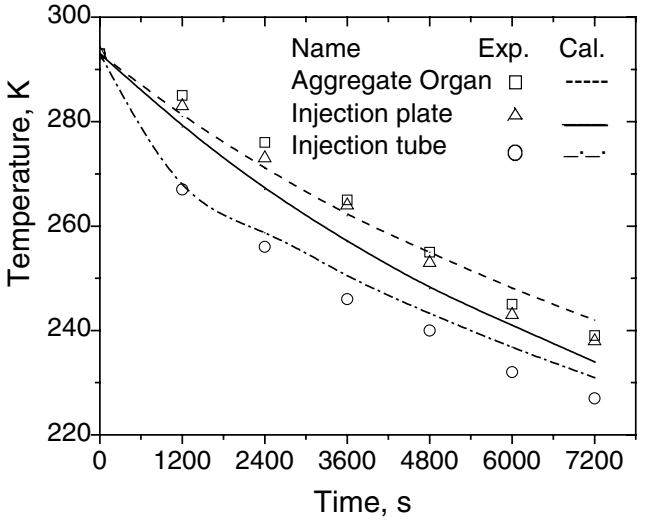

Fig. 9 Temperature comparisons between calculations and experimentations.

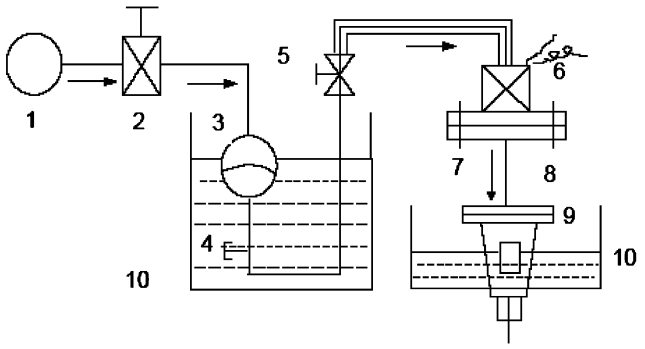

Fig. 10 Scheme of the experimental apparatus.

inside the injection tube is much smaller than that of the exterior coolant, so that the temperature of the injection tube is considered invariable. To compare with the experiment, the front temperature t_{out} of the propellant stream is chosen as the research parameter in the calculation. Because the period it takes for the front propellant stream to flow through the injection tube is very short, so the injection-tube's temperature is considered as the invariable in the filled process. Then, all the conditions in the calculation are the same as those in the experimentation.

The results of the experiment and the calculation are compared in Table 1. At the condition of the injection tube temperature t_{tube} is 213 K and the liquid entry temperatures t_{in} are 253 and 252.8 K. Two test results show that no freezing happens and the simulation liquid flows through the injection tube continuously. The front temperatures t_{out} of the propellant stream shown by the calculation result are 246.1 and 245.9 K; both are higher than the freezing point t_i.

When the injection-tube temperature t_{tube} drops to 207 K, the simulation liquid freezes and the injection tube is blocked in three tests. And as the temperature t_{in} declines, the time that lasted ($\Delta\tau_i$) from the entry of the simulation liquid into the injection tube to the blocking of the injection tube varies from 1 min to instant. On the same conditions (as the experimentations), the results of the simulation calculations are the following: the front temperature t_{out} is 244 K when $t_{in} = 250.8$ K, the propellant stream freezes in the other two times (when t_{in} are 247.1 and 246.5 K), and the axial locations x_i, where the front propellant stream temperature dropped to t_i are 20 and 15 mm, respectively.

In the experiment, the simulation liquid freezes on the inner wall of the injection tube at the beginning, and as the thickness of the ice increases the injection tube is blocked finally. In the calculating model, the temperature difference in the radial direction of the propellant stream is neglected, so the process in which the injection

Table 1 Results of the experimentations and the calculations

Temperature t_{in}, K	Temperature t_{tube}, K	Experimental results	Calculation results
253	213	No freezing	$t_{out} = 246.1$ K
246.5	207	$\Delta\tau_i \approx 0$ s	$x_i = 15$ mm
247.1	207	$\Delta\tau_i = 3$ s	$x_i = 20$ mm
250.8	207	$\Delta\tau_i = 60$ s	$t_{out} = 244$ K
252.8	213	No freezing	$t_{out} = 245.9$ K

tube is blocked could not be shown. But as shown in the calculation, the axial location x_i moves to the entry side of the injection tube indicating that the time period $\Delta\tau_i$ turned short. So the calculation results agree with the experiment.

VII. Conclusions

1) The thermal calculation model and the case analysis of the attitude-control thruster's components in the space cryogenic environment are performed. And the results agree well with that of the simulated experiment carried out in the vacuum cryogenic chamber on the ground.

2) The physical model and mathematical equations are put forward to calculate the propellant stream temperature variation while flowing inside the injection tube of the attitude-control monopropellant thruster in the vacuum cryogenic space. The cryogenic experiments using the head of the thrust chamber show that the calculation model is reliable.

3) For the typical 10 N thruster, the propellant stream will not freeze in the injection tube in the start process if the thruster is started 6 h after the fairing is thrown as long as the initial temperature of the propellant is higher than 263 K.

4) If the front temperature of the propellant stream is higher than the freezing point, the propellant can flow through the injection tube continuously without a freezing accident happening afterward. Three equations are presented to calculate how the front temperature varies with the velocity of the propellant stream, the length, and the inner diameter of the injection tube.

The calculation model and the experimentation results have the reference value to the thermal reliability analysis of the thruster and the fly mission design of the spacecraft.

Acknowledgments

This work was partially supported by the Shanghai Institute of Space Propulsion. The authors thank Zhou Hong-ling and Huang Rui-sheng who are in the Shanghai Institute of Space Propulsion for their help with the experiment.

References

[1] Pang, Z., "Malfunction and Countermeasure of Satellite," *Scientific Chinese*, Vol. 3, May 1996, pp. 41, 42.

[2] Fan, X., Jiang, X., and Huang, W., "Model Based Fault Diagnosis for Satellite Heat Control Subsystem," *Journal of Harbin Institute of Technology*, Vol. 33, No. 3, 2001, pp. 318–325.

[3] Song, L., "Thermal Reliability Design Project of the Attitude-Control Thruster FY-84," Shanghai Institute of Space Propulsion, 1994.

[4] Li, J., "Temperature Calculation of the head of a 10N Thrust Chamber," Shanghai Institute of Space Propulsion, 1995.

[5] Zhou, H., "Vacuum Cryogenic Experimentation Report of the Attitude-Control Thruster FY-84," Shanghai Institute of Space Propulsion, 1995.

[6] Wang, C., Li, M., Tang, J., and Zhou, X., "Thermal Performance Analysis for the Propellant Tank and its Insulator," *Energy and the Environment—Proceedings of the International Conference on Energy and the Environment*, Vol. 1, Shanghai Scientific and Technical Publishers, Shanghai, China, 2003, pp. 938–941.

[7] Zhou, H., "Temperature Drop Investigation of the Monopropellant Thruster in the Space Cryogenic Environment," M.S. Thesis, Aeronautics and Astronautics Department, Shanghai Jiao Tong University, China, 2004.

[8] Travis, K., Todd, B., and Evans, D., "Departure from Navier-Stokes Hydrodynamics in Confined Liquids," *Physical Review E*, Vol. 55, No. 4, 1997, pp. 4288–4295.

[9] Trethway, D., and Meinhart, C., "Apparent Fluid Slip at Hydrophobic Microchannel Walls," *Physics of Fluids*, Vol. 14, No. 3, 2002, pp. L9–L12.

[10] Guo, Z.-Y., and Li, Z.-X., "Size Effect on Microscale Single-Phase Flow and Heat Transfer," *International Journal of Heat and Mass Transfer*, Vol. 46, No. 5, 2003, pp. 149–159.

[11] Sharp, K. V., and Adrian, R. J., "Transition from Laminar to Turbulent Flow in Liquid Filled Microtubes," *Experiments in Fluids*, Vol. 36, No. 1, 2004, pp. 741–747.

[12] Min, G., *Spacecraft Thermal Control Technology*, Satellite Engineering Series, Astronautics and Aeronautics Publishing House, Beijing, 1991, pp. 33, 34.

[13] Yang, X., and Ma, Q., *Radiation Heat Transfer Factor Handbook*, National Defense Industry Publishing House, Beijing, 1982, pp. 45–91.

[14] Weng, J., Pan, Z., and Min, G., "A Method of Calculating External Heat Fluxes on Arbitrary Shaped Convex Surface of Spacecraft," *Chinese Space Science and Technology*, Vol. 14, No. 2, 1994, pp. 11–18.

[15] Sieder, E. N., and Tate, C. E., "Heat Transfer and Pressure Drop of Liquids in Tubes," *Industrial and Engineering Chemistry*, Vol. 28, No. 12, 1936, pp. 1429–1435.